HHS Public Access

Author manuscript

Eur Radiol. Author manuscript; available in PMC 2015 May 07.

Published in final edited form as:

Eur Radiol. 2014 January ; 24(1): 200–208. doi:10.1007/s00330-013-2998-4.

Postoperative pulmonary and aortic 3D haemodynamics in patients after repair of transposition of the great arteries

Julia Geiger,
Department of Radiology, Medical Physics, University Medical Center Freiburg, Hugstetter Str. 55, 79106 Freiburg, Germany

Daniel Hirtler,
Department of Congenital Heart Disease and Paediatric Cardiology, University Medical Center Freiburg-Bad Krozingen, Freiburg, Germany

Jonas Bürk,
Department of Radiology, Medical Physics, University Medical Center Freiburg, Hugstetter Str. 55, 79106 Freiburg, Germany

Brigitte Stiller,
Department of Congenital Heart Disease and Paediatric Cardiology, University Medical Center Freiburg-Bad Krozingen, Freiburg, Germany

Raoul Arnold,
Department of Congenital Heart Disease and Paediatric Cardiology, University Medical Center Heidelberg, Heidelberg, Germany

Bernd Jung,
Department of Radiology, Medical Physics, University Medical Center Freiburg, Hugstetter Str. 55, 79106 Freiburg, Germany

Mathias Langer, and
Department of Radiology, Medical Physics, University Medical Center Freiburg, Hugstetter Str. 55, 79106 Freiburg, Germany

Michael Markl
Department of Radiology, Feinberg School of Medicine, Northwestern University, Chicago, USA. Department Biomedical Engineering, McCormick School of Engineering, Northwestern University, Chicago, USA

Julia Geiger: julia.geiger@uniklinik-freiburg.de

Abstract

Objectives—To characterise aortic and pulmonary haemodynamics and investigate the correlation with post-surgical anatomy in patients with dextro-transposition of the great arteries (d-TGA).

Correspondence to: Julia Geiger, julia.geiger@uniklinik-freiburg.de.

Methods—Four-dimensional (4D) MRI was performed in 17 patients after switch repair of TGA and 12 healthy controls (age, 11.9±5.4 vs 23.3±1.6 years). Patients were divided according to the pulmonary trunk (TP) position in relation to the ascending aorta (AAo): anterior (n =10) and right/left anterior position (n =7). Analysis included visual grading (ranking 0–2) of pulmonary and aortic vortical and helical flow, flow velocity quantification, blood-flow distribution to the right and left pulmonary arteries (flow ratio rPA:lPA), and vessel lumen areas.

Results—Anterior TP position was associated with increased vortices in six out of ten patients compared with right anterior TP position (one out of seven) and controls (none). Reduced systolic lPA and TP lumina in patients resulted in significantly increased peak systolic velocities (P <0.001). Flow ratio rPA:lPA was more heterogeneous in patients (rPA:lPA=1.56 ±0.78 vs volunteers 1.09±0.15; P <0.05) with predominant flow to the rPA. Eleven patients presented increased helices in the AAo (grade 1.6).

Conclusions—Evaluation of post-surgical haemodynamics in TGA patients revealed increased vortical flow for anterior TP position, asymmetric flow and increased systolic flow velocity in the pulmonary arteries owing to reduced vascular lumina.

Keywords

4D MRI; Haemodynamics; D-transposition of the great arteries; Vortices; Pulmonary geometry

Introduction

Dextro-transposition of the great arteries (d-TGA) is a cyanotic congenital heart defect characterised by ventriculoarterial discordance with the aorta originating from the right ventricle and the pulmonary artery from the left ventricle [1]. Standard treatment for d-TGA is the arterial switch operation based on the Jatene principle, which leads to surgical correction of the displaced arteries and transfer of the coronary arteries [2]. In the typical postoperative Lecompte position, the pulmonary trunk is located anterior of the ascending aorta and the pulmonary arteries embrace the ascending aorta [3].

Mid-term and long-term complications include pulmonary arterial stenoses, aortic root dilatation, coronary stenoses and valve insufficiencies after the corrective arterial switch procedure [4–8]. Adult patients demonstrate low mortality but require frequent re-interventions in the right ventricular outflow tract [9]. Regular follow-up imaging by echocardiography and magnetic resonance imaging (MRI) is therefore mandatory [10]. Owing to concerns associated with ionising radiation, cardiac catheterisation and computed tomography (CT) should only be considered as second-choice investigations [11]. Echocardiography can be challenging because of limitations related to the acoustic window, which is affected by the post-surgical retrosternal location of the pulmonary trunk and pulmonary arteries [12]. MRI using standard axial double inversion recovery or multiplanar T2-HASTE sequences such as black blood contrast or steady-state free precession (SSFP) as bright blood sequences is therefore superior and is now the method of choice for depicting the geometry of the cardiovascular system in TGA patients after surgery [13–16]. Pulmonary blood-flow can be evaluated with cine phase contrast (PC) MRI to investigate pulmonary stenoses arising from the altered vessel geometry and morphological vessel

lumen changes during the heart cycle [12]. However, routine two-dimensional (2D) PC imaging is limited to predefined 2D imaging slices and does not permit characterisation of aortic and pulmonary haemodynamics with full volumetric coverage of the d-TGA cardiovascular system.

Time-resolved 3D PC MRI with three-directional velocity encoding (4D flow MRI) has become available for the comprehensive assessment of 3D vascular haemodynamics in patients with aortic lesions and after repair of congenital heart defects [17–25]. The ability of 4D flow MRI to visualise and quantify complex 3D blood-flow patterns has led to deeper understanding of haemodynamics in patients with different types of congenital heart disease [17, 20, 21, 24].

It was the aim of this study to analyse the impact on altered flow characteristics in paediatric patients with d-TGA who had undergone the arterial switch operation many years previously based on whole-heart 4D flow MRI. We compared our findings with aortic and pulmonary haemodynamics in normal control subjects. Our purpose was to test the hypothesis that there is an association between altered aortic and pulmonary flow patterns and the post-surgical anatomy and pulmonary trunk position.

Materials and methods

Patients

Seventeen patients after arterial switch repair for d-TGA (mean age 11.9±5.4 years, range 2–22 years, 11 male) and 12 healthy volunteers (23.3±1.6 years, range 21–26 years, 6 male) underwent whole-heart 4D flow MRI between June 2009 and November 2011. Median age at corrective surgery was 9 days (range 3–18 days). Access to detailed surgical reports was only possible for nine patients. Two patients had an additional ventricular septal defect. The classic Lecompte manoeuvre with the pulmonary arteries encircling the ascending aorta (AAo) was performed in 15 patients. In the two remaining patients, the left pulmonary artery was located posterior to the AAo. Volunteers were recruited from medical students, they were not matched for age and gender. Detailed patients' characteristics are shown in Table 1.

This study was approved by our local ethics committee, and written informed consent was obtained from all participants (or the parents) before the MRI examinations.

Magnetic resonance imaging

MRI examinations of patients were performed at 1.5 T (Magnetom Avanto, Siemens, Germany) using a standard 12-channel body receive coil. Volunteers underwent 3 T MRI (Trio, Siemens, Germany). Patients underwent imaging in the routine diagnostic work-up to evaluate the pulmonary arteries for the presence of stenosis. The routine cardiac MRI protocol consisted of anatomical and cine SSFP sequences as well as time-resolved contrast-enhanced MR angiography (CE-MRA) for depicting perfusion of the pulmonary arteries (Prohance, Bracco, 0.2 mmol/kg body weight, injection rate 1.5–2.0 ml/s). For time-resolved CE-MRA, 20 consecutive 3D data volumes were acquired in a coronal view with a temporal update rate of 2.2–3.5 s, as described previously [26]. Sequence parameters were as follows:

echo time (TE)=1.03–1.1 ms, repetition time (TR)=2.61–2.72 ms, matrix=320×240–270, field of view (FOV)=380–450 mm×285–380 mm, spatial resolution=1.2–1.4×1.2–1.4×1.2–1.4 mm^3, flip angle 25°. Sequence parameters of the sagittal 3D SSFP sequence used to measure the aortic root were: TE = 1.48–1.56 ms, TR=3.3–3.5 ms, matrix=512×352–384, FOV=320–340 mm×240–244 mm, spatial resolution= 0.625–0.66×0.625–0.66×1.2–1.4 mm^3, FA=90°.

In volunteers, the MRI protocol was adapted to the higher magnetic field; gradient-echo and single-shot fast spin echo sequences replaced the SSFP pulse sequences (HASTE). Healthy controls did not undergo CE-MRA.

In all patients and controls, 4D flow MRI data were acquired in sagittal oblique 3D volume individually adapted to include the pulmonary trunk, main pulmonary arteries and thoracic aorta. Measurements were synchronised to the heart rate and respiration using prospective electrocardiographic (ECG) gating and adaptive diaphragm navigator gating [27]. Imaging parameters were as follows: velocity sensitivity=150–200 cm/s, TE=2.3–2.5 ms, TR=4.7–5.1 ms, matrix=128–192×84–104, FOV=225–240 mm×300–380 mm, spatial resolution=1.7–2.5×1.8–2.9×2.5–3.2 mm^3, temporal resolution=37.6–40.8 ms, FA=7°–15°, imaging time ~10–20 min, parallel imaging with reduction factor R =2.

Data analysis: anatomical sequences and CE-MRA

Transverse SSFP images were analysed retrospectively with regard to the postoperative position of the pulmonary trunk (TP) in relation to the AAo. Patients were divided into two groups: (1) TP position straight anterior; (2) TP shifted right or left anterior of the AAo. The TP shift was defined as a TP location deviating by more than 5 mm from an anterior–posterior line (midline) through the centre of the AAo in a transverse image plane as illustrated in Fig. 1. Multi-planar reformations of the sagittal 3D SSFP imaging with diaphragm navigation were used to measure the aortic root diameter. Aortic sinus size was measured in three dimensions as suggested by Burman et al. [28] to conform to the established echocardiographic reference data from the Framingham study [29]. Mean values of all three measurements were calculated and used for comparison with reference values [28, 30]. Aortic root diameters were normalised to body surface area (BSA) and evaluated using nomograms and Z-scores [31]. Z-scores above 2 were categorised as pathological. In volunteers, anatomical assessment of the aortic sinuses was based on two diameter measurements in coronal and sagittal HASTE images.

Time-resolved 3D CE-MRA data were evaluated with regard to temporal differences in the contrast enhancement of the pulmonary peripheral arteries. Asymmetric lung perfusion was defined as delayed contrast medium arrival by at least one 3D CE-MRA time frame in the left or right lung.

Data analysis: 4D flow MRI

Data processing included corrections for eddy currents, Maxwell terms and velocity aliasing as described previously [32]. A 3D phase contrast MR angiogram (PC-MRA) was calculated from the 4D flow MRI data and loaded into commercially available 3D flow visualisation

software (EnSight; CEI, Apex, NC, USA). Pulmonary and aortic blood-flow patterns were visualised using time-resolved 3D particle traces emitted from planes at the level of the aortic and pulmonary valve, the proximal right pulmonary artery (rPA) and left pulmonary artery (lPA). In addition, 3D streamlines representing the 3D distribution of blood-flow velocities at a single time-frame in the cardiac cycle were calculated using the same emitter planes [33]. All traces were colour-coded according to the local blood-flow velocity.

Visual analysis of 3D flow patterns included the evaluation of non-physiological vortical and helical flow patterns in the aorta and pulmonary arteries. Time-resolved 3D particle traces were viewed dynamically for each patient and healthy volunteer in consensus reading by two experienced readers (17 years in total). Vortical flow was defined as regional circular flow patterns deviating by more than 90° from the physiological flow direction along the vessel lumen. Helical flow was defined as a corkscrew-like motion in the direction of the physiological flow. A three-graded ranking scale was used for vortex and helix intensity: no vortex/helix=0, moderate vortex/helix (flow rotation <360°)=1, pronounced vortex/helix (flow rotation >360°)=2.

Blood-flow was quantified in manually-positioned analysis planes in the proximal AAo above the aortic valve, in the TP above the pulmonary valve, and in the middle segment of the rPA and lPA. Vessel lumen contours were manually delineated for all time-frames using custom built software programmed in Matlab (The Mathworks, Natick, MA, USA). Mean velocity-time curves, peak systolic velocity and net flow over the cardiac cycle were calculated for all analysis planes. The lumen segmentation was used to measure the vessel lumen area during peak systolic flow. Each vessel area was normalised to the body surface area (BSA) using the Mosteller equation [31].

Statistics

Continuous variables were reported as mean ± standard deviation. To detect statistically significant differences between continuous variables, unpaired two-sided *t*-tests were applied (Excel, Microsoft). Correlation between vessel lumen area and flow velocity was assessed using linear regression and Pearson correlation coefficient *r* using Graphpad Prism (Graphpad Software, La Jolla, CA, USA). All tests used a significance level of $P < 0.05$.

Results

TGA morphology and vessel areas

The TP was located straight anterior of the AAo in ten patients (TP shift < 5 mm, 1.2 mm ±1.3 mm), right anterior in six patients (TP shift=15.4±7.1 mm), left anterior in one patient (TP shift=22 mm). The mean deviation from the aortic mid-line in the sideward shifted TP group was 16.3±6.9 mm (range 6.5–25 mm). Two patients had a supravalvular TP stenosis, one a valvular stenosis with a distal aneurysm. Stenoses of the pulmonary arteries were detected in two subjects; one patient had a proximal rPA stenosis, one a dissection in the lPA.

All patients displayed significantly altered aortic-root geometry compared with normal controls (mean Z-score=1.7±0.8 vs −0.18±0.85, $P < 0.001$). Five patients had a Z-score

above 2. One volunteer had an aortic root diameter at the upper level of the normal range (Z-score=1.8) and an abnormally angulated, cube-shaped aortic arch.

As summarised in Table 2, normalised systolic vessel lumen area was significantly (P <0.001) reduced for the lPA area in TGA patients compared with controls, while the rPA area was similar. The normalised TP area in TGA patients was also significantly (P <0.001) decreased.

3D blood-flow visualisation

As summarised in Table 3, we detected no vortices in the AAo and TP in any of the healthy volunteers. Conversely, moderate or pronounced vortical flow in the TP was detected in six patients with anterior TP position (mean grade 1.6±0.5), which was absent in patients with a right anterior TP position (Figs. 2 and 3). Pronounced (moderate) vortical flow was seen in four (two) patients. Left anterior TP position resulted in moderate vortical formation. Vortices in the lPA were found in three patients with an anterior TP position (grade 1.3±0.6), in the rPA in two patients with an anterior TP position (grade 2) and one patient with a right anterior TP position (grade 1).

Moderate or pronounced helical flow was seen in the lPA of both patient groups (Fig. 2; 9/17 patients, grade 1.3±0.5), while helical flow was less frequent in the rPA (4/17, grade 1.25±0.5) and TP (3/17, grade 1) groups. Eight controls had helical flow patterns in the rPA which encompassed the complete vessel lumen (grade 1). Compared with the slight physiological right-handed helix in controls, increased systolic helical flow patterns were detected in the AAo (Fig. 4): 11 patients had an abnormal helix not encompassing the complete vessel lumen (mean grade 1.6±0.5). Mild aortic regurgitation was observed in six patients.

Flow quantification

Systolic peak velocity in the TP was significantly higher (P < 0.001) in patients (1.74 m/s ±0.63 m/s) than in controls (0.95 m/s±0.12 m/s). Peak velocity differences were even more pronounced in the rPA (2.04 m/s±0.43 m/s vs 0.98 m/s±0.14 m/s, P <0.001) and the lPA (1.78 m/s±0.54 m/s vs 0.89 m/s±0.13 m/s, P <0.001). Aortic flow velocities were similar in patients (1.35 m/s±0.22 m/s) and volunteers (1.39 m/s±0.23 m/s).

Correlation analysis revealed significant inverse relationships between systolic vessel lumen diameter and peak systolic velocity for the rPA (r =−0.37, P <0.05), lPA (r =−0.44, P <0.05) and TP (r =−0.79, P <0.001).

The rPA:lPA flow ratio was more heterogeneous in patients with a predominant flow to the rPA (flow ratio rPA:lPA=1.56 ±0.78) compared with the control group (rPA:lPA=1.09± 0.15; P <0.05).

Lung perfusion

Time-resolved CE-MRA revealed symmetric contrast medium distribution to both lungs in 12 TGA patients, whereas contrast enhancement of the peripheral left pulmonary arteries was delayed by 2.92±0.53 s (= time needed for the acquisition of one 3D CE-MRA data set)

in five cases (*see* example in Fig. 5) with right anterior TP (n =3) and anterior TP (n =2) position. Noticeably, asymmetric lung perfusion was found in those patients with the highest rPA:lPA flow ratio ranging from 1.69 to 3.69.

Discussion

Four-dimensional flow MRI visualisation and quantification of postoperative blood-flow in a cohort of paediatric d-TGA patients after switch repair revealed several anomalous flow patterns compared with healthy volunteers. The post-surgical TP position was directly associated with changes in pulmonary haemodynamics: we observed enhanced pulmonary vortical flow in association with the haemodynamically unfavourable anterior TP position. In addition, systolic pulmonary blood-flow velocity was increased and the normalised vessel lumen area reduced in all TGA patients independent of TP position. Furthermore, the TGA patients' flow distribution to the right and left lungs demonstrated increased asymmetry as assessed by the quantification of rPA:lPA flow ratios and lung perfusion based on time-resolved CE-MRA.

Common complications such as stenotic supravalvular arteries and narrowing of the pulmonary arteries associated with oval configuration can be depicted and evaluated on multiplanar MRI sequences, as shown in a previous study by Weiss et al. [16]. As cardiac and vessel anatomy is not static, it is important to analyse the dynamic changes in vessel morphology and blood-flow over the cardiac cycle. This can be achieved by cine imaging and flow measurements as shown by Gutberlet et al. [12].

In this study, vessel diameter changes during systole and diastole were examined based on whole-heart cine 4D flow MRI data with full volumetric coverage of the aorta and large pulmonary arteries. To overcome age-related differences caused by non-age-matched volunteers, all parameters were normalised to BSA. We found reduced TP and lPA lumen areas during systole compared with healthy controls. Consistent with results from earlier reports, we speculate that the expansion of the AAo during systole caused an intermittent stenosis of the lPA rather than the rPA owing to the exceptional postoperative anatomy. As expected, temporary pulmonary vessel compression leads to a significant increase in peak velocity in the TP and in both pulmonary arteries in comparison to the healthy volunteer group and to reference values of the pulmonary outflow tract obtained in MRI flow measurements which resulted in an average systolic flow velocity of 66 cm/s [34]. Of note, we observed increased peak systolic velocities even in patients without manifest (supra-) valvular stenosis on anatomical images. A second contributory factor to the higher flow velocities in TGA patients might be related to a phenomenon described by Grotenhuis [35] in 2007 as a result of scar formation at the site of the anastomosis in analogy to observations in patients with repaired coarctation. The vessel loses its distensibility owing to scar tissue, which results in higher flow velocities and subsequent risk of right ventricular hypertrophy.

Similar to previously reported findings by Gutberlet et al. [12], we also detected a significantly reduced vessel lumen area of the patients' lPA during systole, which can be attributed to the aortic dilatation and compression of the adjacent lPA, also in synopsis with the deformed vessel shape (unlike the more round-oval-shaped pulmonary arteries in

volunteers). Conversely, the rPA's vessel area was smaller but not significantly different from that of the volunteer group. A limitation of the 4D flow-based assessment of pulmonary geometry is related to insufficient contrast during diastole owing to slow flow. As a result, vessel contour segmentation was difficult to perform; thus we omitted the diastolic phase from our study's evaluation.

Another main finding was the altered rPA:lPA flow ratio with predominant blood-flow to the right lung. In addition, we observed an association between delayed contrast enhancement of the left lung on time-resolved CE-MRA, which we detected in the five patients with the highest rPA:lPA ratios. We assume that the asymmetric flow distribution could be a result of systolic lPA compression by the aorta leading to predominant flow to the right lung. A potential long-term consequence of the continuous volume overload of one lung is the development of pulmonary hypertension and ventricular impairment.

It should be noted that the arterial switch operation (although termed 'anatomical' repair) does not establish normal cardiovascular geometry. In healthy humans, the aorta and pulmonary artery outlets have a spiral configuration in relation to each other. The Lecompte procedure does not preserve this spiral geometry. After the Lecompte manoeuvre, the TP is frequently compressed between the sternum and the AAo and becomes oval-shaped, which might influence pulmonary blood-flow patterns [36]. In a previous study, Tang and coworkers examined flow models by computational fluid dynamics and detected that velocity in the right ventricular outflow tract and wall-shear stress distribution were more homogeneous in the normal spiral geometry. They recommended restoring the great arteries in a spiral fashion to avoid ineffective blood-flow dynamics [36]. In our study, we found changes in pulmonary haemodynamics due to differences in the post-surgical TP position in relation to the AAo after the Lecompte manoeuvre. Interestingly, there was increased vortical flow in patients with anterior TP position, which was absent in all but one patient with a right anterior TP location. Of note, the one patient with vortical flow and right anterior TP position had a different post-TGA repair configuration with the lPA located posterior to the AAo (i.e. no classical Lecompte manoeuvre). These observations indicate that there might be a tendency towards more physiological flow in association with the right anterior TP position. Regarding normal flow in the TP, we observed a right-handed helical flow pattern in eight healthy volunteers starting in the distal TP with continuity to the rPA, similar to a 4D MRI study by Bächler et al. [37], who described a helical rPA flow in 15 out of 18 volunteers.

Aortic root dilatation as a result of the switch procedure is a common finding, usually associated with only mild valve insufficiency [38–40]. In our study cohort, about one-third of TGA patients had mild aortic valve insufficiency. Their aortic root diameters were greater than in the healthy volunteers. Based on standard nomograms, all patients except the youngest were above the upper second standard deviation [30]. The relatively large standard deviation of the patients' AAo sizes might be due to differences in analysis plane placement in relation to the aortic valve. Planes closer to the aortic valve lead to larger areas because of the aortic root's ectasia. One can assume that the progressive root dilatation is associated with the genuine pulmonary root's different tissue, which expands under systemic pressure conditions as is seen after Ross operations [41]. Another possible explanation is scar

formation at the site of the patches due to transferred coronary arteries. Helical flow in the patients' AAo was clearly enhanced compared with normal volunteers. These findings concur with other studies that revealed abnormal helical flow in the ascending aorta owing to ectasia of the ascending aorta or aortic sinus in patients with Marfan syndrome, or in patients with bicuspid aortic valves [22, 23, 42]. Although aortic root dilatation with mild insufficiency is not considered a critical issue in the current literature, increased helical flow patterns might cause changes in aortic wall shear forces and thus progressive dilatation.

Limitations of our study include the small size of our patient cohort which highlights the feasibility character of our study. Statistical subgroup analysis would benefit from larger patient cohorts. Larger cohorts and, ideally, long-term follow-up studies need to be performed to define a clear relationship between post-interventional TGA geometry and haemodynamic outcome. An obvious link between the observed geometric and flow alterations and the real patient outcome cannot be proven without longitudinal studies. Another limitation is the different magnetic field strengths (3 T for volunteer examinations and 1.5 T for the patient studies). The reason for this is the availability of devices in our department. The patients underwent MRI at the children's hospital, which is located far from the main hospital. In our experience, the lower magnetic field strength did not result in impaired image quality or flow evaluation. The age difference between the patients and the volunteers is another limitation of our study which is based on legal issues which restrict investigation of healthy children and adolescents for research purposes.

It was not the aim of this study to compare the 4D data with reference 2D data; this has already been the subject of a previous study [43]. Correct placement of the 2D planes is challenging in post-surgical abnormally running pulmonary arteries, including the risk of incorrect flow quantification. A comparison with echocardiographic data was not possible because of the frequently impaired echocardiographic pulmonary arterial evaluation. The detected systolic pulmonary artery stenoses were not considered to be critical enough to be treated by immediate catheter angiography; only the patient with lPA dissection was treated with a stent.

In conclusion, MRI plays an important role in the post-surgical long-term follow-up of d-TGA patients after arterial switch repair. Four-dimensional MRI enables the visualisation and quantification of altered post-surgical pulmonary and aortic haemodynamics. Our results suggest that a disadvantageous anterior pulmonary trunk position may exert a geometric effect and thus trigger pulmonary blood-flow alterations. High pulmonary flow velocities correlated with reduced vessel lumen areas. Asymmetric flow to the right and left pulmonary arteries due to systolic lPA compression revealed asymmetric perfusion of the left and right lungs. Four-dimensional MRI may thus have the potential to identify the optimal postoperative vessel anatomy to avoid distorted flow and to help the surgeon find the best pulmonary trunk position to reduce re-interventions in the pulmonary arteries.

Acknowledgments

This work was undertaken with grant support from the National Heart, Lung, And Blood Institute of the National Institutes of Health under Award Number R01HL115828.

Abbreviations

AAo	Ascending aorta
lPA	Left pulmonary artery
PC	Phase contrast
rPA	Right pulmonary artery
TP	Pulmonary trunk

References

1. Martins P, Castela E. Transposition of the great arteries. Orphanet J Rare Dis. 2008; 3:27. [PubMed: 18851735]
2. Jatene AD, Fontes VF, Paulista PP, et al. Anatomic correction of transposition of the great vessels. J Thorac Cardiovasc Surg. 1976; 72:364–370. [PubMed: 957754]
3. Lecompte Y, Zannini L, Hazan E, et al. Anatomic correction of transposition of the great arteries. J Thorac Cardiovasc Surg. 1981; 82:629–631. [PubMed: 7278356]
4. Massin MM, Nitsch GB, Däbritz S, Seghave MC, Messmer BJ, von Bernuth G. Growth of pulmonary artery after arterial switch operation for simple transposition of the great arteries. Eur J Pediatr. 1998; 157:95–100. [PubMed: 9504780]
5. McMahon CJ, Ravekes WJ, O'Brian Smith E, et al. Risk factors for neo-aortic root enlargement and aortic regurgitation following arterial switch operation. Pediatr Cardiol. 2004; 25:329–335. [PubMed: 14727099]
6. Hutter PA, Kreb DL, Mantel SF, Hitchcock JF, Meijboom EJ, Bennink GB. Twenty-five years' experience with arterial switch operation. J Thorac Cardiovasc Surg. 2002; 124:790–797. [PubMed: 12324738]
7. De Koning WB, van Osch-Grevers M, Ten Harkel AD, et al. Follow-up outcomes 10 years after arterial switch operation for transposition of the great arteries: comparison of cardiological health status and health-related quality of life to those of a normal reference population. Eur J Pediatr. 2008; 167:995–1004. [PubMed: 17987315]
8. Fricke TA, d'Udekem Y, Richardson M, et al. Outcomes of the arterial switch operation for transposition of the great arteries: 25 years of experience. Ann Thorac Surg. 2012; 94:139–145. [PubMed: 22607787]
9. Kempny A, Wustmann K, Borgia F, et al. Outcome in adult patients after arterial switch operation for transposition of the great arteries. Int J Cardiol. 201210.1016/j.ijcard.2012.06.066
10. Warnes CA. Transposition of the great arteries. Circulation. 2006; 114:2699–2709. [PubMed: 17159076]
11. Achenbach S, Barkhausen J, Beer M, et al. Consensus recommendations of the German Radiology Society (DRG), the German Cardiac Society (DGK) and the German Society for Pediatric Cardiology (DGPK) on the use of cardiac imaging with computed tomography and magnetic resonance imaging. Rofo. 2012; 184:345–368. [PubMed: 22426867]
12. Gutberlet M, Boeckel T, Hosten N, et al. Arterial switch procedure for D-transposition of the great arteries: quantitative mid-term evaluation of hemodynamic changes with cine MR imaging and phase-shift velocity mapping—initial experience. Radiology. 2000; 214:467–475. [PubMed: 10671595]
13. Blakenberg F, Rhee J, Hardy C, Helton G, Higgins SS, Higgins CB. MRI vs echocardiography in the evaluation of the Jatene procedure. J Comput Assist Tomogr. 1994; 18:749–754. [PubMed: 8089324]
14. Hardy CE, Helton GJ, Kondo C, Higgins SS, Young NJ, Higgins CB. Usefulness of magnetic resonance imaging for evaluating great-vessel anatomy after arterial switch operation for D-transposition of the great arteries. Am Heart J. 1994; 128:326–332. [PubMed: 8037100]

15. Cohen MD, Johnson T, Ramrakhiani. MRI of surgical repair of transposition of the great arteries. AJR Am J Roentgenol. 2010; 191:250–260. [PubMed: 20028930]
16. Weiss F, Habermann CR, Lilje C, et al. MRI of pulmonary arteries in follow-up after arterial-switch-operation (ASO) for transposition of the great arteries (d-TGA). Rofo. 2005; 177:849–855. [PubMed: 15902635]
17. Markl M, Geiger J, Kilner PJ, et al. Time-resolved three-dimensional magnetic resonance velocity mapping of cardiovascular flow paths in volunteers and patients with Fontan circulation. Eur J Cardiothorac Surg. 2011; 39:206–212. [PubMed: 20598560]
18. Geiger J, Markl M, Jung B, et al. 4D-MR flow analysis in patients after repair for tetralogy of Fallot. Eur Radiol. 2011; 21:1651–1657. [PubMed: 21720942]
19. Markl M, Geiger J, Jung B, Hirtler D, Arnold R. Noninvasive evaluation of 3D hemodynamics in a complex case of single ventricle physiology. J Magn Reson Imaging. 2012; 35:933–937. [PubMed: 22271353]
20. Uribe S, Bächler P, Valverde I, Crelier GR, Beerbaum P, Tejos C, Irarrazaval P. Hemodynamic assessment in patients with one-and-a-half ventricle repair revealed by four-dimensional flow magnetic resonance imaging. Pediatr Cardiol. 2013; 34:447–451. [PubMed: 22447380]
21. Francois CJ, Srinivasan S, Schiebler ML, et al. 4d cardiovascular magnetic resonance velocity mapping of alterations of right heart flow patterns and main pulmonary artery hemodynamics in tetralogy of fallot. J Cardiovasc Magn Reson. 2012; 14:16. [PubMed: 22313680]
22. Hope MD, Hope TA, Meadows AK, et al. Bicuspid aortic valve: four-dimensional MR evaluation of ascending aortic systolic flow patterns. Radiology. 2010; 255:53–61. [PubMed: 20308444]
23. Barker AJ, Markl M, Bürk J, et al. Bicuspid aortic valve is associated with altered wall shear stress in the ascending aorta. Circ Cardiovasc Imaging. 2012; 5:457–466. [PubMed: 22730420]
24. Valverde I, Nordmeyer S, Uribe S, et al. Systemic-to-pulmonary collateral flow in patients with palliated univentricular heart physiology: measurement using cardiovascular magnetic resonance 4d velocity acquisition. J Cardiovasc Magn Reson. 2012; 14:25. [PubMed: 22541134]
25. Sundareswaran KS, Haggerty CM, de Zelicourt D, et al. Visualization of flow structures in fontan patients using 3-dimensional phase contrast magnetic resonance imaging. J Thorac Cardiovasc Surg. 2012; 143:1108–1116. [PubMed: 22088274]
26. Frydrychowicz A, Bley TA, Zadeh Z, et al. Image analysis in time-resolved large field of view 3D MR-angiography at 3T. J Magn Reson Imaging. 2008; 28:1116–1124. [PubMed: 18972352]
27. Markl M, Harloff A, Bley TA, et al. Time-resolved 3D MR velocity mapping at 3T: improved navigator-gated assessment of vascular anatomy and blood flow. J Magn Reson Imaging. 2007; 25:824–831. [PubMed: 17345635]
28. Burman ED, Keegan J, Kilner P. Aortic root measurement by cardiovascular magnetic resonance. Circ Cardiovasc Imaging. 2008; 1:104–113. [PubMed: 19808527]
29. Vasan RS, Larson MG, Benjamin EJ, Levy D. Echocardiographic reference values for aortic root size: the Framingham Heart Study. J Am Soc Echocardiogr. 1995; 8:793–800. [PubMed: 8611279]
30. Gautier M, Detaint D, Fermanian C, et al. Nomograms for aortic root diameters in children using two-dimensional echocardiography. Am J Cardiol. 2010; 105:888–894. [PubMed: 20211339]
31. Mosteller RD. Simplified calculation of body-surface area. N Engl J Med. 1987; 317:1098. [PubMed: 3657876]
32. Bock J, Frydrychowicz A, Stalder AF, et al. 4d phase contrast MRI at 3T: effect of standard and blood-pool contrast agents on SNR, PC-MRA, and blood flow visualization. Magn Reson Med. 2010; 63:330–338. [PubMed: 20024953]
33. Buonocore MH. Visualizing blood flow patterns using streamlines, arrows, and particle paths. Magn Reson Med. 1998; 40:210–226. [PubMed: 9702703]
34. Abolmaali ND, Esmaeili A, Feist P, et al. Reference values of MRI flow measurements of the pulmonary outflow tract in healthy children. Rofo. 2004; 176:837–845. [PubMed: 15173976]
35. Grotenhuis HB, Kroft LJM, van Elderen SGC, et al. Right ventricular hypertrophy and diastolic dysfunction in arterial switch patients without pulmonary artery stenosis. Heart. 2007; 93:1604–1608. [PubMed: 17277348]

36. Tang T, Chiu I-S, Chen H-C, Cheng K-Y, Chen S-J. Comparison of pulmonary arterial flow phenomena in spiral and Lecompte models by computational fluid dynamics. J Thorac Cardiovasc Surg. 2001; 122:529–534. [PubMed: 11547306]

37. Bächler P, Pinochet N, Sotelo J, Crelier G, Irarrazaval P, Tejos C, Uribe S. Assessment of normal flow patterns in the pulmonary circulation by using 4D magnetic resonance velocity mapping. Magn Reson Imaging. 2013; 31:178–188. [PubMed: 22898700]

38. Angeli E, Raisky O, Bonnet D, Sidi D, Vouhé PR. Late reoperations after neonatal arterial switch operation for transposition of the great arteries. Eur J Cardiothorac Surg. 2008; 34:32–36. [PubMed: 18468448]

39. Losay J, Touchot A, Capderou A, et al. Aortic valve regurgitation after arterial switch operation for transposition of the great arteries: incidence, risk factors, and outcome. J Am Coll Cardiol. 2006; 47:2057–2062. [PubMed: 16697325]

40. Schwartz ML, Gauvreau K, del Nido P, Mayer J, Colan SD. Long-term predictors of aortic root dilatation and aortic regurgitation after arterial switch operation. Circulation. 2004; 110:128–132. [PubMed: 15197143]

41. Pees C, Laufer G, Michel-Behnke I. Similarities and differences of the aortic root after arterial switch and Ross operation in children. Am J Cardiol. 2013; 111:125–130. [PubMed: 23062315]

42. Geiger J, Markl M, Herzer L, et al. Aortic flow patterns in patients with Marfan syndrome assessed by flow-sensitive 4D MRI. J Magn Reson Imaging. 2012; 35:594–600. [PubMed: 22095635]

43. Stalder AF, Russe MF, Frydrychowicz A, Bock J, Hennig J, Markl M. Quantitative 2D and 3D phase contrast MRI: optimized analysis of blood flow and vessel wall parameters. Magn Reson Med. 2008; 60:1218–1231. [PubMed: 18956416]

Key Points

- 3D phase contrast MRI with velocity encoding (4D MRI) has numerous cardiovascular applications
- 4D MRI demonstrates postoperative haemodynamics following surgery for transposition of the great arteries
- Flow visualisation depicted enhanced pulmonary vortices in the anterior pulmonary trunk
- Narrow pulmonary arterial systolic lumina resulted in increased peak systolic velocities

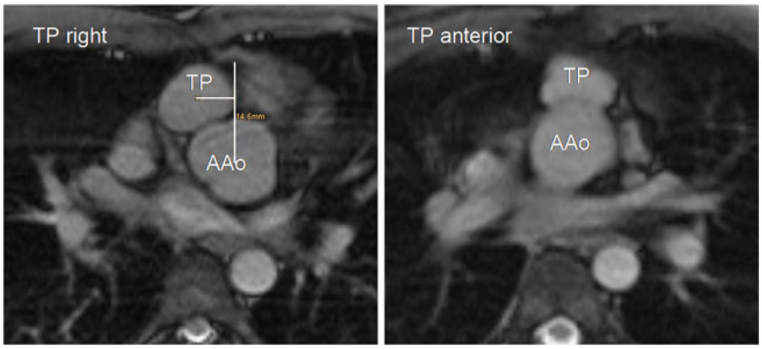

Fig. 1.

Transverse steady-state free precession (SSFP) image of a patient after arterial switch repair depicting anatomy of the pulmonary trunk (*TP*) in relation to the ascending aorta (*AAo*). **a** TP shift to the right anterior position measured in comparison to a line in anterior–posterior direction through the centre of the AAo. **b** TP in straight anterior position in relation to the AAo

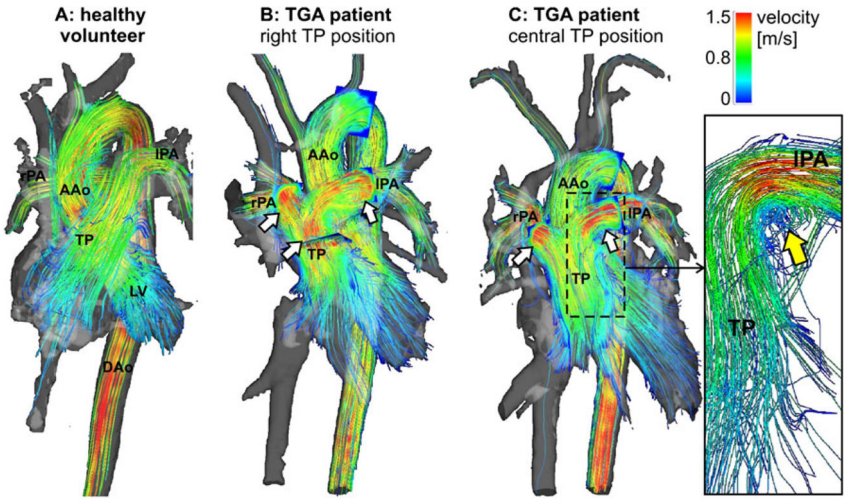

Fig. 2.

Overview of 3D haemodynamics in healthy volunteers (**a**) compared with TGA patients visualised by colour-coded streamlines. High systolic flow velocity in the pulmonary trunk (*TP*) and pulmonary arteries are visible in both patients (**b**, **c**). **c** Vortical flow at the transition of the TP to the left pulmonary artery (*lPA*) in a TGA patient with straight anterior TP position. *LV* left ventricle, *AAo* ascending aorta, *DAo* descending aorta

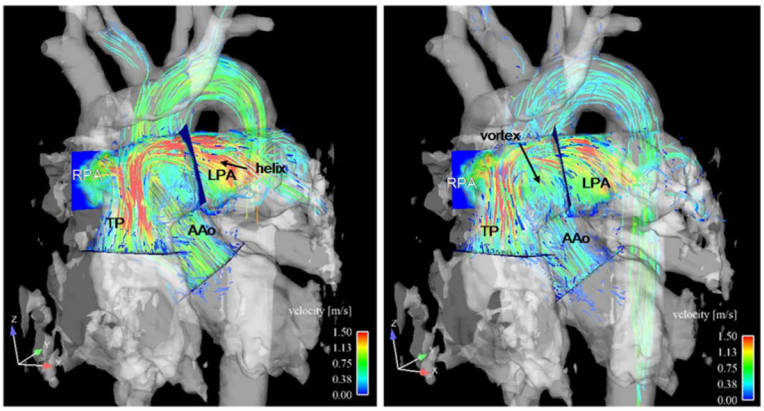

Fig. 3.

Helical and vortical formation in the pulmonary trunk (*TP*) and left pulmonary artery (*lPA*) in a TGA patient with anterior TP position during early (*left*) and late (*right*) systole visualised by 3D particle traces emitted from the level of the pulmonary valve. *AAo* ascending aorta

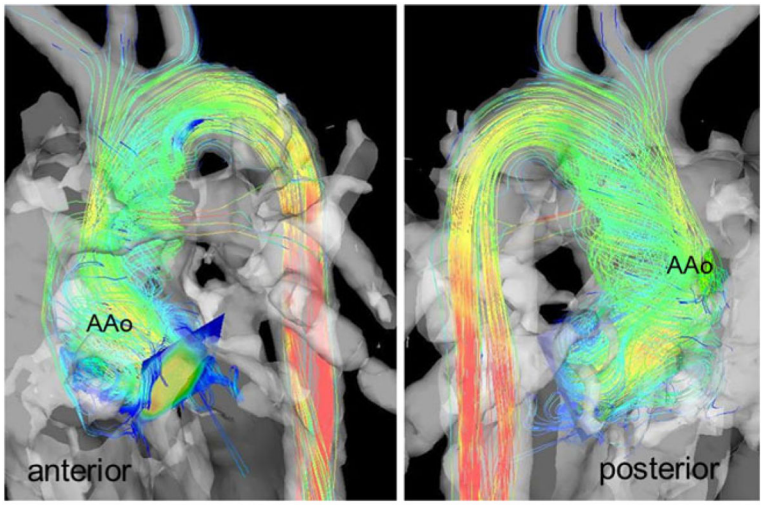

Fig. 4.

Helical flow patterns in the ascending aorta (*AAo*) during systole visualised by colour-coded streamlines, *anterior* and *posterior* views

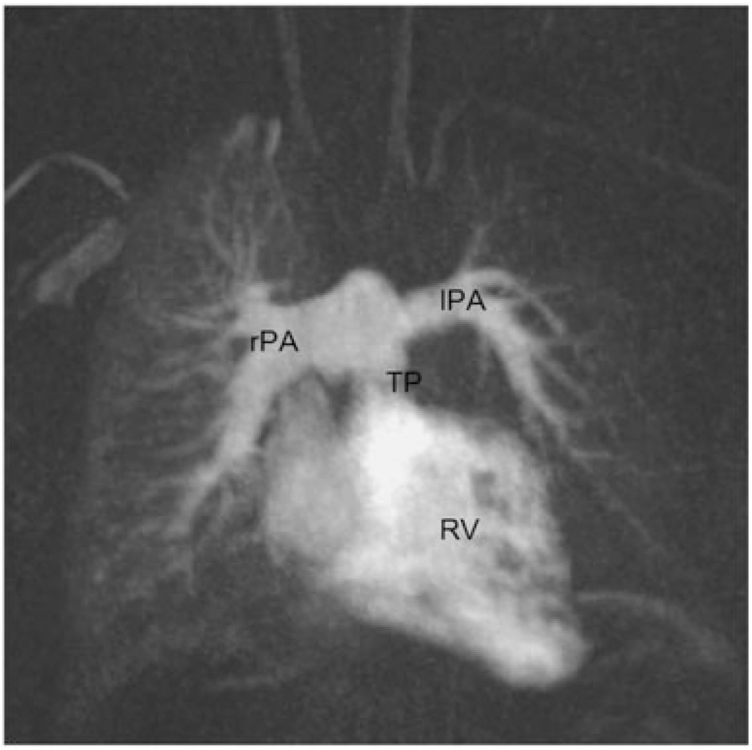

Fig. 5.
Contrast-enhanced MRA detects asymmetric contrast enhancement of the right and left lungs with delayed perfusion of the left peripheral pulmonary arteries without the presence of left pulmonary artery (*lPA*) stenosis. *RV* right ventricle, *TP* pulmonary trunk, *rPA* right pulmonary artery

Table 1

Body characteristics of all patients and volunteers listed in the chronological order of MRI examination for each group

Patients	Age (years)	Sex	Height (m)	Weight (kg)	BSA
1	2	m	0.92	12	0.55
2	16	m	1.69	66	1.76
3	15	m	1.69	63	1.72
4	22	m	1.78	73	1.90
5	10	f	1.43	35	1.18
6	13	m	1.58	39	1.31
7	6	f	1.26	25	0.94
8	15	m	1.55	41	1.33
9	8	m	1.36	28	1.03
10	10	m	1.49	34	1.19
11	22	f	1.62	57	1.60
12	8	m	1.36	27	1.01
13	9	m	1.44	27	1.04
14	15	f	1.64	65	1.72
15	10	m	1.38	40	1.24
16	14	f	1.63	53	1.55
17	7	f	1.24	21	0.85
Volunteers					
1	25	f	1.77	63	1.76
2	25	m	1.90	92	2.20
3	22	f	1.75	65	1.78
4	21	m	1.80	78	1.97
5	25	m	1.79	70	1.87
6	22	f	1.73	57	1.66
7	26	f	1.77	65	1.79
8	23	m	1.73	65	1.77
9	24	m	1.73	63	1.74
10	22	f	1.68	54	1.59

Patients	Age (years)	Sex	Height (m)	Weight (kg)	BSA
11	23	m	1.80	60	1.73
12	22	f	1.66	54	1.58

m male, *f* female, *BSA* body surface area

Table 2

Vessel lumen area diameters normalised to BSA in TGA patients and volunteers

Areas normalised to BSA (mm^2/m^2)	TGA patients	Volunteers	*P* value
TP	239±68	346±64	< **0.001**
rPA	118±42	144±23	0.05
lPA	97±30	167±40	< **0.001**
AAo	293±106	231±46	0.04

BSA body surface area, *TGA* transposition of the great arteries, *TP* pulmonary trunk, *rPA* right pulmonary artery, *lPA* left pulmonary artery, *AAo* ascending aorta

Table 3

Blood-flow regarding the TP position in relation to the AAo

		Anterior TP *n* =10	**Right anterior TP *n* =6**	**Left anterior TP *n* =1**	**Controls *n* =12**
Age at MRI (years)		10.5±4.4	12.5±5.8	22	23.3±1.6
Vortices in TP	0	4	5		12
	1	2	1	1	0
	2	4	0		0
Helices in TP	0	8	5	1	12
	1	2	1		0
	2	0	0		0
Aortic root dilatation Z >2		7	4	1	0
Vortices in AAo	0	10	6		12
	1	0	0	1	0
	2	0	0		0
Helices in AAo	0	3	0		12
	1	4	1		0
	2	3	3	1	0
TP regurgitation		2	2	0	0
Ao regurgitation		4	2	0	0

TP pulmonary trunk, *AAo* ascending aorta, *n* number

0 = no vortex/helix, *1* = moderate vortex/helix (flow rotation <360°), *2* = pronounced vortex/helix (flow rotation >360°)